Structure of Redox Intercalated $(NH_4)_{0.5}V_2O_5 \cdot mH_2O$ Xerogel Using the Pair Distribution Function Technique

Pantelis N. Trikalitis,† Valeri Petkov,‡ and Mercouri G. Kanatzidis*,†

Department of Chemistry and Center for Fundamental Materials Research, Michigan State University, East Lansing, Michigan 48824, and Department of Physics, Central Michigan University, Mt. Pleasant, Michigan 48859

Received February 12, 2003. Revised Manuscript Received June 10, 2003

The structure of $(NH_4)_{0.5}V_2O_5 \cdot mH_2O$ ($m \approx 0.9$), a representative member of the family of intercalated solids with reduced V_2O_5 xerogel framework, has been successfully determined using the atomic pair distribution function (PDF) technique. We show that at the atomic scale $(NH_4)_{0.5}V_2O_5 \cdot mH_2O$ is isostructural with pristine $V_2O_5 \cdot nH_2O$ that features a double layer of V_2O_5 separated by water molecules and ammonium ions in a monoclinic unit cell (space group $C2/m$) with parameters $a = 11.845(1)$ Å, $b = 3.677(1)$ Å, $c = 9.058(1)$ Å, and $\beta = 88.635°$. Vanadium oxide network in $(NH_4)_{0.5}V_2O_5 \cdot mH_2O$ is slightly expanded when compared to that in pristine $V_2O_5 \cdot nH_2O$, reflecting the elongation of V−O bonds in the former material. The results presented here prove that the redox intercalation of $V_2O_5 \cdot nH_2O$ xerogel is indeed a topotactic reaction.

Introduction

Vanadium oxide xerogel, $V_2O_5 \cdot nH_2O$, has been known for more than a century as a highly reactive material with a diverse and rich intercalation chemistry demonstrated by numerous cation-exchange, acid−base, and redox reactions.[1,2] The layered structure and the redox intercalation ability of the xerogel allow insertion of various intercalant species. Perhaps the most fascinating and spectacular reactions of this type involve the in-situ intercalation-polymerization of organic molecules such as aniline, pyrrole, and thiophene, and the formation of conducting polymers within the lamellar inorganic host.[3−7] Polymer-intercalated vanadium xerogel composites are currently being investigated for potential applications in high-energy density rechargeable batteries.[8−12]

The redox intercalation of $V_2O_5 \cdot nH_2O$ xerogel involves a process in which the layers become partially reduced and cationic molecules insert between them resulting in the formation of bronze-type materials.[2−7,13−23] The intercalated materials are highly disordered over long ranges and do not crystallize, yet they are well ordered on the short and intermediate scales. Spectroscopic and X-ray data from pristine and intercalated systems have suggested that the insertion processes are topotactic meaning that the insertion of guest molecules does not change the host structure considerably.[9,14,16,19,22,24] The suggestion, however, has never been quantitatively proven, partly because the 3-D structure of pristine $V_2O_5 \cdot nH_2O$ xerogel had remained unknown for decades.

Recently, the 3-D structure of $V_2O_5 \cdot nH_2O$ was solved by employing the atomic pair distribution function (PDF) technique. The xerogel was found to be an assembly of almost perfect bilayers of square pyramidal VO_5 units, separated by water molecules.[25] Studies on the atomic arrangement in bronze-type materials obtained by intercalating of $V_2O_5 \cdot nH_2O$ with molecular

* To whom correspondence should be addressed. kanatzid@cem.msu.edu.
† Michigan State University.
‡ Central Michigan University.

(1) Livage, J.; Pelletier, O.; Davidson, P. *J. Sol-Gel Sci. Technol.* **2000**, *19*, 275−278.
(2) Livage, J. *Chem. Mater.* **1991**, *3*, 578−593.
(3) Kanatzidis, M. G.; Wu, C. G.; Marcy, H. O.; Kannewurf, C. R. *J. Am. Chem. Soc.* **1989**, *111*, 4139−4141.
(4) Kanatzidis, M. G.; Wu, C. G.; Marcy, H. O.; Degroot, D. C.; Kannewurf, C. R. *Chem. Mater.* **1990**, *2*, 222−224.
(5) Liu, Y. J.; Degroot, D. C.; Schindler, J. L.; Kannewurf, C. R.; Kanatzidis, M. G. *Adv. Mater.* **1993**, *5*, 369−372.
(6) Liu, Y. J.; Degroot, D. C.; Schindler, J. L.; Kannewurf, C. R.; Kanatzidis, M. G. *J. Chem. Soc.-Chem. Commun.* **1993**, 593−596.
(7) Wu, C. G.; DeGroot, D. C.; Marcy, H. O.; Schindler, J. L.; Kannewurf, C. R.; Liu, Y. J.; Hirpo, W.; Kanatzidis, M. G. *Chem. Mater.* **1996**, *8*, 1992−2004.
(8) Chen, W.; Xu, Q.; Hu, Y. S.; Mai, L. Q.; Zhu, Q. Y. *J. Mater. Chem.* **2002**, *12*, 1926−1929.
(9) Oliveira, H. P.; Graeff, C. F. O.; Rosolen, J. M. *Mater. Res. Bull.* **1999**, *34*, 1891−1903.
(10) Shouji, E.; Buttry, D. A. *Langmuir* **1999**, *15*, 669−673.
(11) Prosini, P. P.; Passerini, S.; Vellone, R.; Smyrl, W. H. *J. Power Sources* **1998**, *75*, 73−83.
(12) Goward, G. R.; Leroux, F.; Nazar, L. F. *Electrochim. Acta* **1998**, *43*, 1307−1313.
(13) Liu, Y. J.; Degroot, D. C.; Schindler, J. L.; Kannewurf, C. R.; Kanatzidis, M. G. *Chem. Mater.* **1991**, *3*, 992−994.
(14) Liu, Y. J.; Cowen, J. A.; Kaplan, T. A.; Degroot, D. C.; Schindler, J.; Kannewurf, C. R.; Kanatzidis, M. G. *Chem. Mater.* **1995**, *7*, 1616−1624.
(15) Liu, Y. J.; Schindler, J. L.; DeGroot, D. C.; Kannewurf, C. R.; Hirpo, W.; Kanatzidis, M. G. *Chem. Mater.* **1996**, *8*, 525−534.
(16) Park, N. G.; Ryu, K. S.; Park, Y. J.; Kang, M. G.; Kim, D. K.; Kang, S. G.; Kim, K. M.; Chang, S. H. *J. Power Sources* **2002**, *103*, 273−279.
(17) Guerra, E. M.; Brunello, C. A.; Graeff, C. F. O.; Oliveira, H. P. *J. Solid State Chem.* **2002**, *168*, 134−139.
(18) Millet, M.; Farcy, J.; Pereira-Ramos, J. P.; Sabbar, E. M.; De Roy, M. E.; Besse, J. P. *Solid State Ion.* **1998**, *112*, 319−327.
(19) Yatabe, T.; Nakano, M.; Matsubayashi, G. E. *J. Mater. Chem.* **1998**, *8*, 699−703.
(20) Ackermans, B.; Schoonheydt, R. A.; RuizHitzky, E. *J. Chem. Soc.-Faraday Trans.* **1996**, *92*, 4479−4484.
(21) Judeinstein, P.; Sanchez, C. *J. Mater. Chem.* **1996**, *6*, 511−525.
(22) Mori, M.; Isobe, T.; Senna, M. *Solid State Ionics* **1995**, *81*, 157−163.
(23) Watanabe, T.; Shimizu, A.; Inagaki, M. *J. Mater. Chem.* **1995**, *5*, 753−756.
(24) Rojas-Cervantes, M. L.; Casal, B.; Aranda, P.; Saviron, M.; Galvan, J. C.; Ruiz-Hitzky, E. *Colloid Polym. Sci.* **2001**, *279*, 990−1004.

10.1021/cm030173y CCC: $25.00 © 2003 American Chemical Society
Published on Web 08/01/2003

species are scarce. Here we employ the PDF technique to determine the structure of the prototypical bronze-type material $(NH_4)_{0.5}V_2O_5{\cdot}mH_2O$ with partially reduced $[V_2O_5]^{x-}$ layers. We give unequivocal proof that the redox intercalation of $V_2O_5{\cdot}nH_2O$ xerogel is a topotactic reaction and discuss the effect of added electrons to the vanadium−oxide network. Thus we give another demonstration of the great potential of the PDF technique in determining the atomic structures of poorly diffracting and nanocrystalline materials.[26,27]

Experimental Section

Preparation of $V_2O_5{\cdot}nH_2O$ Xerogel. The $V_2O_5{\cdot}nH_2O$ xerogel was prepared by dissolution of crystalline V_2O_5 in concentrated H_2O_2 (30%). Typically, 4 g of crystalline V_2O_5 powder, purchased from Aldrich, was dissolved in 250 mL of concentrated hydrogen peroxide (30%) at room temperature. A strong exothermic reaction occurred after about 20 min, and a dark red solution formed which spontaneously transformed into a dark red gel. The gel was cast on a glass plate and allowed to dry at room temperature until a dark red film was formed. The film was peeled off the glass and used as obtained. This method yields a high quality $V_2O_5{\cdot}nH_2O$ ($n \approx 1.8$) xerogel sample as confirmed by X-ray diffraction, thermogravimetric analysis (TGA), and infrared (IR) measurements in full agreement with previous reports.[1−7]

Preparation of $(NH_4)_{0.5}V_2O_5{\cdot}mH_2O$. The $V_2O_5{\cdot}nH_2O$ xerogel in film form (1 g, 6.67 mmol) was added to 50 mL of acetonitrile with stoichiometric amount of NH_4I. The mixture was refluxed under N_2 atmosphere for 4 h. The dark blue product, which retained the film form, was washed extensively with acetonitrile and dried under vacuum. The composition $(NH_4)_{0.5}V_2O_5{\cdot}mH_2O$ ($m \approx 0.9$) was determined from elemental C, H, N and thermogravimetric (TGA) analyses. This product was ground into a fine powder for the diffraction experiments.

X-ray Diffraction Experiment. The synchrotron X-ray diffraction experiments measurements were carried out at the BESSRC-CAT 11-ID-C beam line at the Advanced Photon Source, Argonne. The sample was carefully packed between Kapton foils to avoid texture formation and subjected to measurements with X-rays of energy 114.67 keV ($\lambda = 0.1081$ Å). The higher energy X-rays were used to extend the range of diffraction data (i.e., to obtain data at higher wave vectors $Q = 4\pi\sin\theta/\lambda$) which is important for the success of PDF analysis. Scattered radiation was collected with an intrinsic germanium detector coupled to a multichannel analyzer. Several runs were conducted and the resulting XRD patterns were averaged to improve the statistical accuracy and to reduce any systematic effect due to instabilities in the experimental setup.

PDF Analysis of the Diffraction Data. A description of the data analysis and extraction of the experimental PDFs has been published in detail elsewhere.[25]

Results and Discussion

The NH_4^+ ion intercalated xerogel was prepared in acetonitrile via a heterogeneous redox reaction in which the solid $V_2O_5{\cdot}nH_2O$ xerogel was reduced with I^- ions as follows

$$V_2O_5{\cdot}nH_2O + 0.5\ NH_4I \rightarrow (NH_4)_{0.5}V_2O_5{\cdot}mH_2O + 0.25\ I_2$$

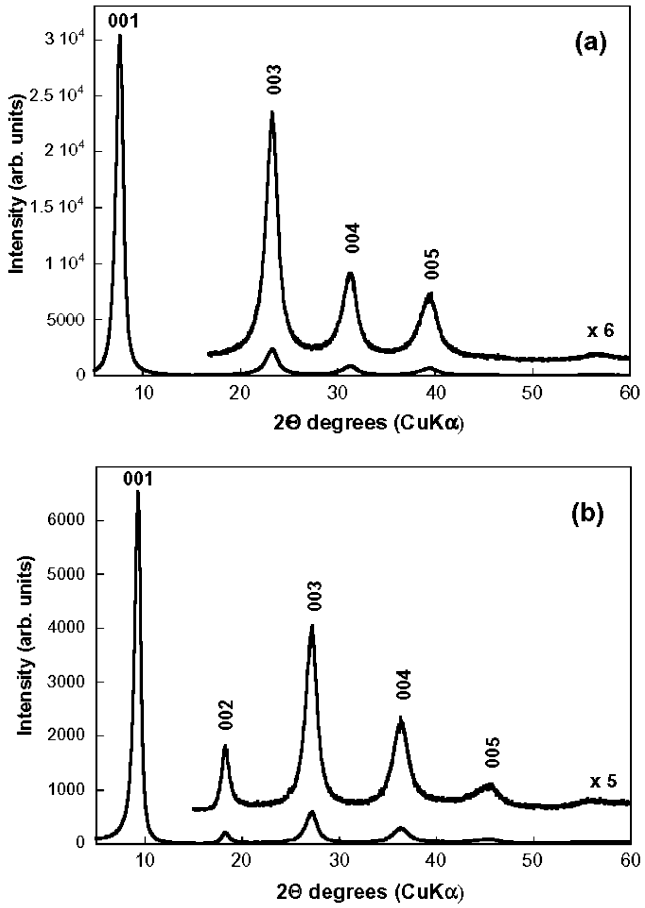

Figure 1. Powder XRD pattern of (a) $V_2O_5{\cdot}nH_2O$ xerogel ($n \approx 1.8$) and (b) $(NH_4)_{0.5}V_2O_5{\cdot}mH_2O$ ($m \approx 0.9$). The data were obtained in reflection geometry.

In this process the xerogel is always a solid, and upon reduction electrons delocalize over the entire V_2O_5 network making it negatively charged. Electrostatic forces then act simultaneously to drive the positive NH_4^+ ions into the structure, expelling water molecules. Upon reduction the material becomes dark blue due to the creation of V^{4+} (d^1 configuration) centers. Interestingly, it also invariably turns brittle regardless of the guest species.

Figure 1 shows X-ray diffraction patterns for $(NH_4)_{0.5}V_2O_5{\cdot}mH_2O$ and $V_2O_5{\cdot}nH_2O$ xerogels obtained in reflection mode. Few strong Bragg peaks of the (*00l*) type dominate the patterns indicating that the layered structure of the $V_2O_5{\cdot}nH_2O$ precursor is preserved in the product of the intercalation reaction. The first strong (*00l*) peak corresponds to the interlayer spacing. It decreases from 11.5 Å in pristine $V_2O_5{\cdot}nH_2O$ to 9.4 Å in the intercalated $(NH_4)_{0.5}V_2O_5{\cdot}mH_2O$ material. The contraction of the interlayer separation is due to the loss of water being replaced by ammonium ions and to the attractive electrostatic interactions between the intercalated NH_4^+ cations and the negatively charged V_2O_5 layers. The same behavior has been observed in $Cs_xV_2O_5{\cdot}nH_2O$.[14] Selected area electron diffraction (SAED) measurements[28] also suggest that the layered-type framework

(25) Petkov, V.; Trikalitis, P. N.; Bozin, E. S.; Billinge, S. J. L.; Vogt, T.; Kanatzidis, M. G. *J. Am. Chem. Soc.* **2002**, *124*, 10157−10162.

(26) Petkov, V.; Billinge, S. J. L.; Larson, P.; Mahanti, S. D.; Vogt, T.; Rangan, K. K.; Kanatzidis, M. G. *Phys. Rev. B* **2002**, *65*, art. no.092105.

(27) Petkov, V.; Billinge, S. J. L.; Heising, J.; Kanatzidis, M. G. *J. Am. Chem. Soc.* **2000**, *122*, 11571−11576.

(28) Selected area electron diffraction (SAED) measurements were performed on a JEOL 120CX transmission electron microscope operating at 120 kV using 150-cm camera length. The samples in film form were firmly crushed using a mortar and pestle and cast on a copper carbon-coated grid.

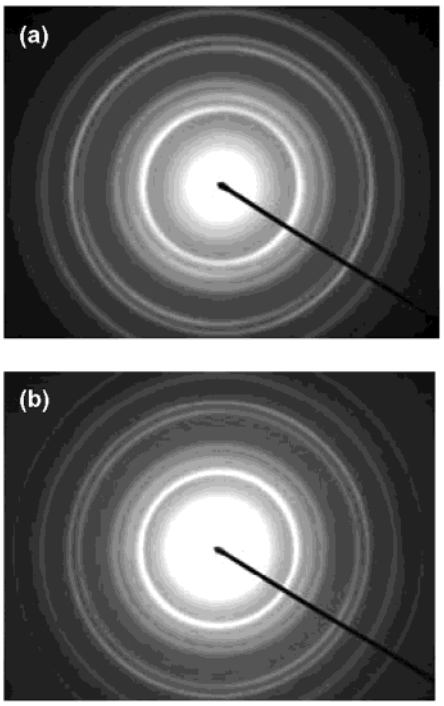

Figure 2. Representative selected area electron diffraction images of (a) $V_2O_5 \cdot nH_2O$ xerogel and (b) $(NH_4)_{0.5}V_2O_5 \cdot mH_2O$. The electron beam is perpendicular to the layers (flat ribbon). The observed diffraction rings originate from the well-defined atomic ordering along the ribbons.

of the pristine xerogel is preserved upon the intercalation of NH_4^+ ions. Figure 2 shows such SAED images for the pristine and ammonium intercalated xerogel. Several well-defined diffraction rings with very similar reciprocal spacing are observed in the images suggesting that the two materials share similar structural features.

Shown in Figure 3 are synchrotron powder diffraction patterns of $(NH_4)_{0.5}V_2O_5 \cdot mH_2O$ and pristine $V_2O_5 \cdot nH_2O$[25] collected in transmission geometry. The materials in film form were ground to powder prior to the analysis to minimize the effect of the film texture in the diffraction pattern and possibly small local stoichiometric variations. As a result the patterns collected in transmission mode are less sensitive to texture effects and representative of the bulk of the samples. The transmission XRD patterns also exhibit the Bragg-like features at low values of wave vectors Q seen in the SAED patterns. In addition, a pronounced diffuse component (see inset in Figure 3) is seen at high Q values. The scarcity of Bragg peaks in the XRD patterns renders them unusable for structure determination by conventional crystallographic approaches such as the Rietveld technique. That is why the diffraction patterns were explored in real space in terms of the corresponding atomic PDFs. The frequently used atomic PDF, also called $G(r)$, is defined as follows:

$$G(r) = 4\pi r[\rho(r) - \rho_o] \qquad (1)$$

where $\rho(r)$ and ρ_o are the local and average atomic number densities, respectively, and r is the radial distance. $G(r)$ gives the number of atoms in a spherical shell of unit thickness at a distance r from a reference atom. It peaks at characteristic distances separating pairs of atoms and thus reflects the atomic structure.

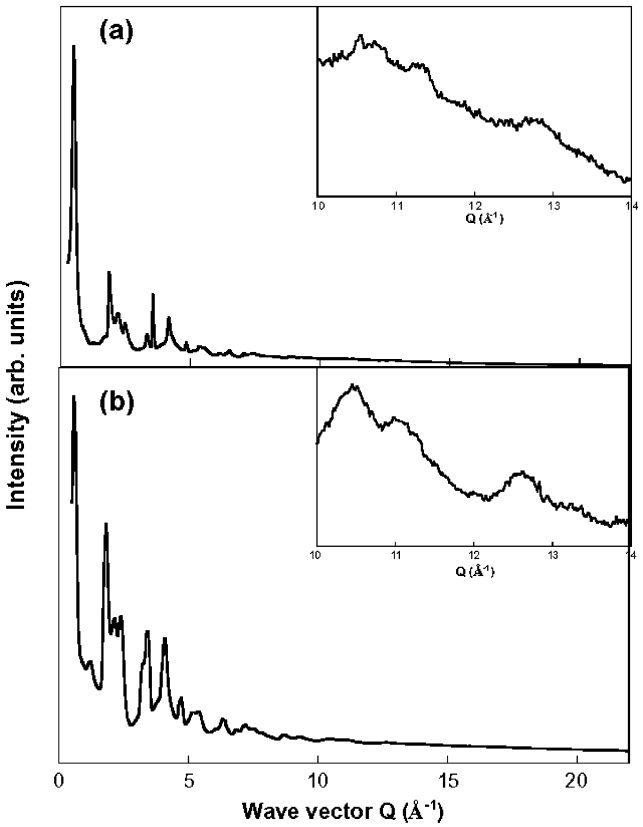

Figure 3. X-ray diffraction patterns of (a) $V_2O_5 \cdot nH_2O$ xerogel and (b) $(NH_4)_{0.5}V_2O_5 \cdot mH_2O$ obtained in transmission geometry ($\lambda = 0.1081$ Å). The high-Q portion of the data, which contains key structural information, is given on an expanded scale in the inset.

$G(r)$ is the Fourier transform of the experimentally observable total structure function, $S(Q)$, i.e.,

$$G(r) = (2/\pi) \int_{Q=o}^{Q_{max}} Q[S(Q) - 1]\sin(Qr)dQ \qquad (2)$$

where Q is the magnitude of the wave vector ($Q = 4\pi\sin\theta/\lambda$). The structure function is related to the coherent part of the powder diffraction pattern of the material as follows:

$$S(Q) = 1 + [I^{coh}(Q) - \sum c_i|f_i(Q)|^2]/|\sum c_i f_i(Q)|^2 \qquad (3)$$

where $I^{coh}(Q)$ is the coherent scattering intensity per atom in electron units and c_i and f_i are the atomic concentration and X-ray scattering factor, respectively, for the atomic species of type i.[25−27,29]

It has been repeatedly shown [25−27,29−36] that the PDF approach is advantageous in the case of materials with

(29) Petkov, V.; Jeong, I. K.; Chung, J. S.; Thorpe, M. F.; Kycia, S.; Billinge, S. J. L. *Phys. Rev. Lett.* **1999**, *83*, 4089−4092.
(30) Billinge, S. J. L.; Proffen, T.; Petkov, V.; Sarrao, J. L.; Kycia, S. *Phys. Rev. B* **2000**, *62*, 1203−1211.
(31) Petkov, V.; Billinge, S. J. L.; Shastri, S. D.; Himmel, B. *Phys. Rev. Lett.* **2000**, *85*, 3436−3439.
(32) Petkov, V.; Jeong, I. K.; Mohiuddin-Jacobs, F.; Proffen, T.; Billinge, S. J. L.; Dmowski, W. *J. Appl. Phys.* **2000**, *88*, 665−672.
(33) Jeong, I. K.; Mohiuddin-Jacobs, F.; Petkov, V.; Billinge, S. J. L.; Kycia, S. *Phys. Rev. B* **2001**, *6320*, art. no. 205202.
(34) Petkov, V.; Billinge, S. J. L.; Shastri, S. D.; Himmel, B. *J. Non-Cryst. Solids* **2001**, *293*, 726−730.
(35) Petkov, V.; Billinge, S. J. L. *Physica B* **2001**, *305*, 83−89.
(36) Petkov, V.; Billinge, S. J. L.; Vogt, T.; Ichimura, A. S.; Dye, J. L. *Phys. Rev. Lett.* **2002**, *89*, art. no. 075502.

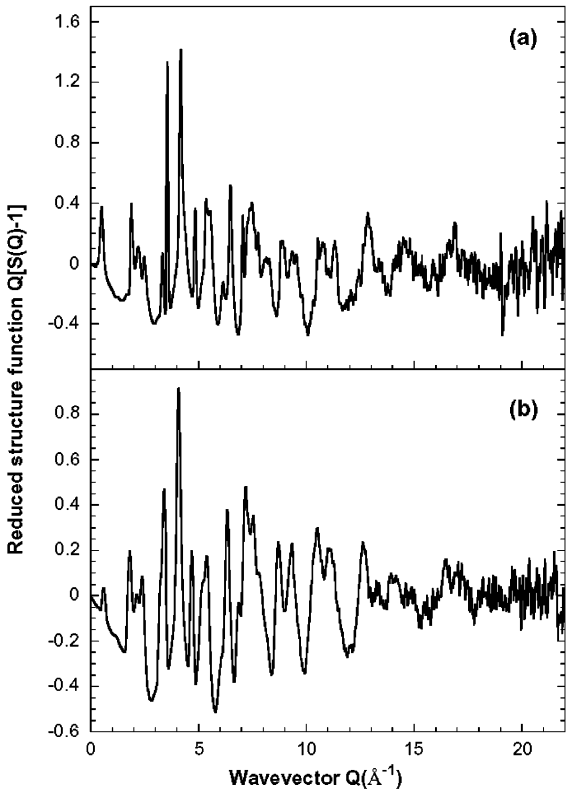

Figure 4. Reduced structure functions, $Q[S(Q)-1]$, of (a) $V_2O_5 \cdot nH_2O$ xerogel and (b) $(NH_4)_{0.5}V_2O_5 \cdot mH_2O$ derived from the XRD patterns of Figure 3.

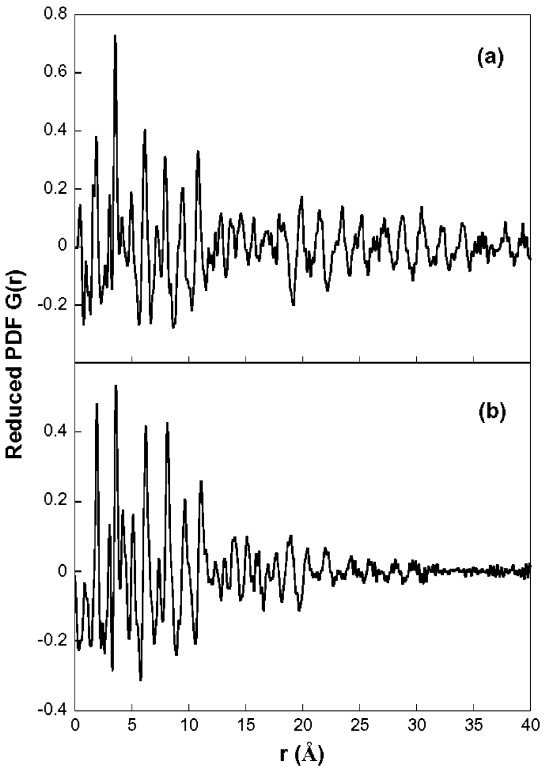

Figure 5. Experimental PDFs for (a) $V_2O_5 \cdot nH_2O$ xerogel and (b) $(NH_4)_{0.5}V_2O_5 \cdot mH_2O$ obtained by Fourier transforming the structure functions of Figure 4.

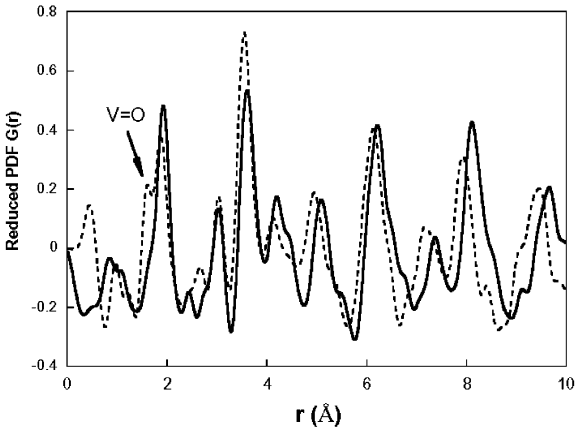

Figure 6. Comparison between the experimental PDFs for $(NH_4)_{0.5}V_2O_5 \cdot mH_2O$ (full line) and $V_2O_5 \cdot nH_2O$ (broken line) xerogel. The comparison clearly shows the expansion of the V_2O_5 network, seen as a systematic shift in the positions of the PDF peaks, upon the redox intercalation of pristine $V_2O_5 \cdot nH_2O$ with ammonium ions.

significant structural disorder exhibiting poor diffraction patterns such as that shown in Figures 1 and 3. The most important advantage is that the PDF reflects both the long-range atomic structure, manifested in the sharp Bragg peaks, and the local structural imperfections, manifest in the diffuse components of the diffraction data. Also, it does not imply any periodicity, rendering the technique particularly useful for highly disordered and nanocrystalline materials with limited structural coherence.

Experimental reduced structure functions ($Q[S(Q)-1]$) extracted from the powder diffraction data of Figure 3 and their Fourier counterparts, the atomic PDFs, $G(r)$, are shown in Figures 4 and 5, respectively. The PDFs of pristine and ammonium intercalated $V_2O_5 \cdot nH_2O$ exhibit similar features, especially in the range 2 Å $< r <$ 10 Å, reflecting the similarity in the atomic arrangement of the two materials. Some differences are, however, also seen. The PDF of $(NH_4)_{0.5}V_2O_5 \cdot mH_2O$ is shifted to higher r values as compared to that of pristine xerogel, suggesting that the average V−O bond length and, hence, the entire V_2O_5 network, in the intercalated material is somewhat expanded. This network expansion becomes more and more obvious as the radial distance r increases (see Figure 6) as the V−O bond-lengths contribute cumulatively to the interatomic vectors seen as peaks in the PDFs.

In addition, the experimental PDF for $(NH_4)_{0.5}V_2O_5 \cdot mH_2O$ decays to zero already at distances $r \approx 30$ Å, whereas that of pristine $V_2O_5 \cdot nH_2O$ xerogel oscillates up to interatomic vectors of ~50 Å.[25] This shows that both pristine $V_2O_5 \cdot nH_2O$ and $(NH_4)_{0.5}V_2O_5 \cdot mH_2O$ are ordered only at nanometer length scales and the structural coherence length is shorter in the intercalated material. The additional structural disorder in $(NH_4)_{0.5}V_2O_5 \cdot mH_2O$ is most probably introduced by the loss of water and intercalation of NH_4^+ ions.

Given the similarities between the SAED and PDF data for pristine and ammonium intercalated xerogels we considered the structure of the former[25] as a starting model for that of the latter material. The structure of pristine $V_2O_5 \cdot nH_2O$ features V_2O_5 bilayers stacked along the c axis of a monoclinic unit cell (space group $C2/m$) with parameters $a = 11.722(3)$ Å, $b = 3.570(3)$ Å, and $c = 11.520(3)$ Å, and $\beta = 88.65°$. To account for the fact that the interlayer distance in the intercalated material $(NH_4)_{0.5}V_2O_5 \cdot mH_2O$, as measured by the posi-

Table 1. Atomic Positions (*x,y,z*) and Anisotropic Thermal Factors, of *V*, *O*, and *N* in Monoclinic $(NH_4)_{0.5}V_2O_5 \cdot mH_2O$ Space Group *C*2/*m* with Lattice Parameters $a = 11.845(1)$ Å, $b = 3.677(1)$ Å, $c = 9.058(1)$ Å, and $\beta = 88.635°$ Obtained by PDF-Based Refinement

atom	*x*	*y*	*z*	U_{11} and U_{22} (Å^2)	U_{33} (Å^2)
V(1)	0.930(1)	0	0.167(1)	0.006(1)	0.117(1)
V(2)	0.229(1)	0	0.174(1)	0.006(1)	0.117(1)
O(1)	0.389(1)	0	0.146(1)	0.012(1)	0.065(1)
O(2)	0.082(1)	0	0.110(1)	0.012(1)	0.065(1)
O(3)	0.758(1)	0	0.104(1)	0.012(1)	0.065(1)
O(4)	0.954(1)	0	0.355(1)	0.012(1)	0.065(1)
O(5)	0.212(1)	0	0.365(1)	0.012(1)	0.065(1)
N[a] or O[a]	0.610(1)	0	0.490(1)	0.012(1)	0.065(1)

[a] Corresponds to NH_4^+ ions and H_2O molecules between the V_2O_5 bilayers.

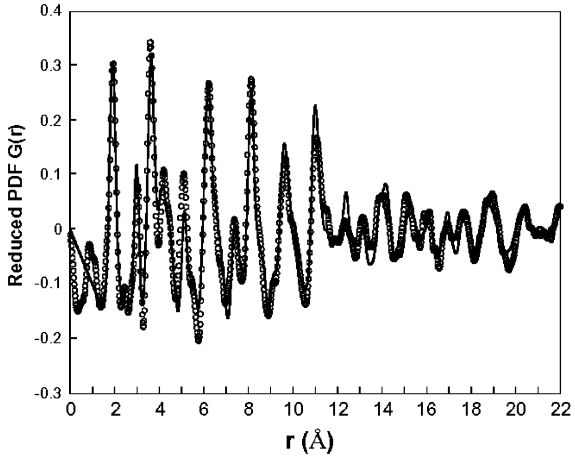

Figure 7. Experimental (symbols) and fitted (solid line) PDFs for $(NH_4)_{0.5}V_2O_5 \cdot mH_2O$. The value of the corresponding goodness-of-fit indicator R_G, as defined in refs 25, 27, and 37, is 31%.

tion of the first peak in the powder diffraction pattern (see Figures 1b and 3b), is 9.4 Å we shortened the *c* parameter of the unit cell from 11.72 Å to 9.4 Å and adjusted the *z*-coordinates of all the atoms in the trial structural model accordingly. The intercalated ammonium ions and water molecules were placed between the V_2O_5 bilayers as they occur in pristine xerogel. This starting model was refined against the experimental PDF data by a least-squares procedure observing the constraints of the space group *C*2/*m*. The program PDFFIT[37] was employed in the refinement. The refined lattice parameters, atomic positions, and thermal factors are summarized in Table 1. Thus, the refined structure model reproduces very well the experimental PDF data as can be seen in Figure 7. The success of the refinement demonstrates that $(NH_4)_{0.5}V_2O_5 \cdot mH_2O$ is essentially isostructural with its precursor, pristine $V_2O_5 \cdot nH_2O$ xerogel, and with that of crystalline δ-$Ag_xV_2O_5$.[38]

A section of the refined structure of $(NH_4)_{0.5}V_2O_5 \cdot mH_2O$ is shown in Figure 8. Similarly to $V_2O_5 \cdot nH_2O$, the ammonium intercalated material is an assembly of double V_2O_5 layers made up of square pyramidal VO_5 units encapsulating the water molecules and ammonium ions. The oxygen coordination of V atoms in $(NH_4)_{0.5}V_2O_5 \cdot mH_2O$ is similar to that in pristine xerogel,

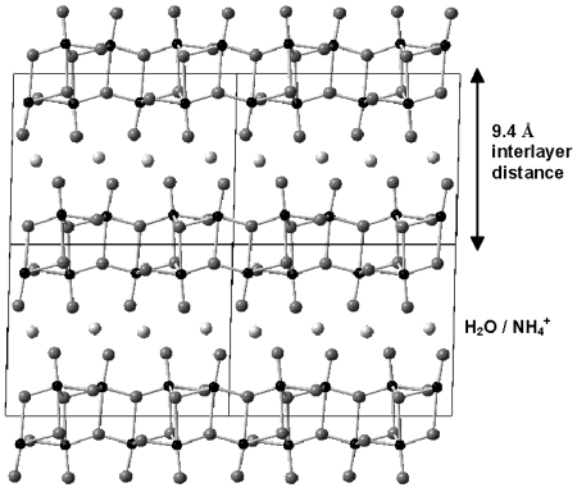

Figure 8. Section of the structure of $(NH_4)_{0.5}V_2O_5 \cdot mH_2O$ as revealed by the PDF analysis. Water and ammonium ions are shown in light gray.

resembling a square pyramid with four oxygen atoms at distances from 1.86 to 2.12 Å making the base of the pyramid and an oxygen atom at ~1.7 Å capping the pyramid that amounts to a V=O double bond. The existence of the latter was confirmed by infrared spectroscopy showing a characteristic absorption at ~980 cm^{-1}. This absorption band is sensitive to intercalation and, in full agreement with previous results,[14] is red shifted compared to the V=O stretching vibration (~1000 cm^{-1}) in pristine xerogel.[14] These distinct V−O bonds in the square pyramidal VO_5 units are the main contributors to the peak around 2 Å in the experimental PDF (Figure 6). In notable contrast, in the pristine xerogel these V−O bonds are differentiated enough to give a resolved split-up first peak in the experimental PDF, where the shortest vector is due to the V=O double bond at 1.6 Å (Figure 6). These results suggest that in $(NH_4)_{0.5}V_2O_5 \cdot mH_2O$ the V=O double bond lengthens, resulting in a more uniform bond-length distribution within the VO_6 octahedra. A possible explanation is as follows: In many d^0 transition metal oxides, as for example in all known modifications of V_2O_5, short V=O double bonds are known to form. The phenomenon is known as second-order Jahn−Teller distortion of octahedral 'Metal-O_6'/d^0 units in metals of high oxidation state. When, however, the metal atoms centering the octahedral unit become reduced (e.g. from V^{5+} to V^{4+}) their radius increases and the V=O bond lengthens, leading to a less distorted VO_6 octahedron. The lengthening of the V=O bonds is mainly due to the fact that the d orbitals of V^{5+} are predominantly antibonding in character and tend to reduce the bond order when populated with electrons to form V^{4+}. This also lessens the Jahn−Teller distortion of the V−O octahedral units and they become more regular in shape.

The weaker bonds within the intercalated $[V_2O_5]^{x-}$ framework, coupled with the increased disorder and decreased coherence length (noted above), is likely the origin of the observed mechanical brittleness of all redox intercalated V_2O_5 materials.

It is also worth noting that the structure of nanocrystalline $(NH_4)_{0.5}V_2O_5 \cdot mH_2O$ bears a strong similarity to that of the recently reported crystalline $(CH_3NH_3)_{0.37}V_2O_5 \cdot 0.33H_2O$.[26] The latter material is not a

(37) Proffen, T.; Billinge, S. J. L. *J. Appl. Crystallogr.* **1999**, *32*, 572−575.
(38) Andersson, S. *Acta Chem. Scand.* **1965**, *19*, 1371−1375.

product of intercalation reaction. It was synthesized hydrothermally and its structure was solved and refined by using the powder diffraction data and the conventional Rietveld method.[39,40]

Another interesting point that deserves to be mentioned is the ability of $V_2O_5 \cdot nH_2O$ xerogels to coordinate to a small amount of water via some V atoms. This ability has been suggested for some time and also observed by NMR experiments.[41] It implies that a tiny fraction of the V atoms are accessible to coordination by water. Although, as the present structural study shows, there is no vanadium−water coordination in the bulk of pristine and intercalated xerogels, it still could occur at the edges of the nanoribbons (~100 Å wide and μm in length) that make up these nanocrystalline materials. At this point it is not known whether in addition to becoming dispersed, the nanoribbons also hydrolyze upon swelling in water. If such a process takes place the nanoribbons may be ripped along their length producing yet narrower ribbons and exposing more V atoms to water. To answer this question we are initiating a study of the structure of dispersed V_2O_5 gels.

Conclusions

The structure of $(NH_4)_{0.5}V_2O_5 \cdot mH_2O$ ($m \approx 0.9$) was determined using the PDF technique and found to be similar to that of pristine $V_2O_5 \cdot nH_2O$ xerogel. Accordingly, at the atomic level the structure features double layers of V_2O_5 stacked along the *c*-axis of a monoclinic unit cell and separated by water molecules and ammonium ions. The results fully demonstrate that the redox intercalation reaction of $V_2O_5 \cdot nH_2O$ xerogel with NH_4I (and by extension all other guest species) is indeed topotactic. Given that $(NH_4)_{0.5}V_2O_5 \cdot mH_2O$ is completely intractable using conventional powder crystallographic techniques such as Rietveld, an important outcome of the results reported here is that PDF analysis yields the correct atomic structure of a highly disorder material such as $(NH_4)_{0.5}V_2O_5 \cdot mH_2O$ in terms of only a few meaningful parameters and demonstrates that it works beyond the limits of traditional crystallography. Moreover, it is necessary to point out here that other powerful characterization techniques such as MAS NMR failed to address the correct structure for $V_2O_5 \cdot nH_2O$ xerogel. Pruski and co-workers[41] very recently reported the investigation of $V_2O_5 \cdot nH_2O$ gels using ^{17}O and 3QMAS NMR. According to their findings they proposed what now must be considered an incorrect structure for $V_2O_5 \cdot nH_2O$ gels: one that features single layers made of VO_5 units between which reside water molecules. Given the new information, resulting from the PDF-based structure determinations of pristine and intercalated $V_2O_5 \cdot nH_2O$ xerogels, the NMR experiments will need to be re-interpreted.

Acknowledgment. Thanks to M. Beno and Y. Ren for the help with the synchrotron experiments. The work was supported by NSF Grant CHE-0211029. Use of the Advanced Photon Source and BESSRC facility was supported by the U. S. Department of Energy, Office of Science, Office of Basic Energy Sciences, under Contract W-31-109-Eng-38. M.G.K. thanks the Guggenheim Foundation for a Fellowship.

CM030173Y

(39) Chen, R. J.; Zavalij, P. Y.; Whittingham, M. S.; Greedan, J. E.; Raju, N. P.; Bieringer, M. *J. Mater. Chem.* **1999**, *9*, 93−100.

(40) Chirayil, T.; Zavalij, P. Y.; Whittingham, M. S. *Chem. Mater.* **1998**, *10*, 2629−2640.

(41) Fontenot, C. J.; Wiench, J. W.; Schrader, G. L.; Pruski, M. *J. Am. Chem. Soc.* **2002**, *124*, 8435−8444.